

Longitudinal Resting-State fMRI Study: A Seed-Based Connectivity Analysis in Patients with Ischemic Stroke and Intracerebral Hemorrhage

Seth B. Boren

Institute for Stroke and Cerebrovascular Diseases and Department of Neurology, McGovern Medical School, The University of Texas Health Science Center at Houston

Sean I. Savitz

Institute for Stroke and Cerebrovascular Diseases and Department of Neurology, McGovern Medical School, The University of Texas Health Science Center at Houston

Timothy M. Elimore

The City College of New York, Department of Psychology

Christin Silos

Institute for Stroke and Cerebrovascular Diseases and Department of Neurology, McGovern Medical School, The University of Texas Health Science Center at Houston

Sarah George

Institute for Stroke and Cerebrovascular Diseases and Department of Neurology, McGovern Medical School, The University of Texas Health Science Center at Houston

Maria A. Parekh

Institute for Stroke and Cerebrovascular Diseases and Department of Neurology, McGovern Medical School, The University of Texas Health Science Center at Houston

Octavio D. Arevalo

Louisiana State University Health Science Center, Department of Radiology

Muhammad E. Haque (✉ Muhammad.E.Haque@uth.tmc.edu)

Institute for Stroke and Cerebrovascular Diseases and Department of Neurology, McGovern Medical School, The University of Texas Health Science Center at Houston

Research Article

Keywords: Ischemic Stroke, Intracerebral Hemorrhage, Resting-State Functional Magnetic Resonance Imaging, Serial Neuroimaging Study.

Posted Date: August 18th, 2021

DOI: <https://doi.org/10.21203/rs.3.rs-806451/v1>

License:  This work is licensed under a Creative Commons Attribution 4.0 International License.

[Read Full License](#)

Abstract

The primary aim of the research was to compare the impact of post-ischemic and hemorrhagic stroke on brain connectivity and recovery using resting-state functional magnetic resonance imaging (rsfMRI). We serially imaged 20 stroke patients, ten with ischemic (IS) and 10 with intracerebral hemorrhage (ICH), at 1, 3, and 12 months after ictus. Data from ten healthy volunteers were obtained from a publically available imaging dataset. All functional and structural images underwent standard processing for brain extraction, realignment, serial registration, unwrapping, and de-noising using SPM12. A seed-based group analysis using CONN software was used to evaluate the Default Mode (DMN) and the Sensorimotor Network (SMN) connections by applying bivariate correlation and hemodynamic response function (hrf) weighting. In comparison to healthy controls (HC), both IS and ICH exhibited disrupted interactions (decreased connectivity) between these two networks at 1M. Interactions then increased by 12M in each group. Temporally, each group exhibited a minimal increase in connectivity at 3M as compared to 12M. Overall, the ICH patients exhibited a greater magnitude of connectivity disruption compared to IS patients, despite a significant intra-subject reduction in hematoma volume. We did not observe any significant correlation between change in connectivity and recovery as measured on the National Institute Stroke Scale (NIHSS) at any time point. These findings demonstrate that largest changes in functional connectivity occur earlier (3M) rather than later (12M) and show subtle differences between IS and ICH during recovery and should be explored further in larger samples.

Introduction

Stroke is the number one cause of disability with about six hundred thousand newly reported stroke cases in the US annually. About 87% of all strokes are ischemic and 13% hemorrhagic (1, 2). Despite significant differences in pathophysiology between ischemic and hemorrhagic stroke, severe to mild disabilities develop in most survivors. Patients with intracerebral hemorrhage (ICH) have a higher risk of fatality and about half of them die within the first month (3). ICH not only causes tissue damage but also leads to secondary injuries such as cellular toxicity, expansion of cytotoxic and vasogenic edema causing an increase in intracranial pressure, tissue compression, and impaired coagulation. Conceptually, it is believed that ICH survivors past the acute stage have better neurological and functional prognoses than patients with ischemic stroke (4, 5), but the literature is contradictory (6). There are several key prognostic factors such as stroke severity, age, lesion volume, location, presence of a mass effect, midline shift, etc., that are relevant to functional outcome (7).

Recently, several task-based and resting-state functional MRI (rs-fMRI) studies have been applied to evaluate post-stroke recovery (8–12). fMRI relies on the magnetic properties of oxyhemoglobin and deoxyhemoglobin to detect localized changes in blood flow caused by neuronal activity. The fMRI signal is known as the blood-oxygen-level-dependent [BOLD] response which can be localized and quantified (13). Since most stroke survivors cannot follow the commands or perform a task during imaging, resting-state fMRI (rs-fMRI), which evaluates neuronal connectivity at rest, has emerged as a method of choice. A wide variety of neurological disorders have been investigated with rsfMRI as a non-invasive tool to track

progression or regression of neurological diseases. (14–17). Previous connectivity studies on stroke survivors have revealed that the effects of damage can extend beyond the area of the stroke lesion (18, 19).

The default mode network (DMN) and sensorimotor network (SMN) of the brain have emerged as the two most reliable networks for assessing connectivity during stroke recovery (20–23). The DMN is the baseline functional network when a subject is not engaged in a specific task and includes the medial temporal lobe, medial prefrontal cortex, posterior cingulate cortex, ventral precuneus, and parietal cortex regions (24, 25). The DMN disengages with other networks during a goal-oriented task and reflects as negatively correlated with various resting-state networks. The sensory-motor network (SNM) includes the primary motor (precentral gyrus), supplementary motor, and somatosensory (postcentral gyrus) regions. Slight engagement of motor functions such as twitches and shuffling can briefly disengage the connectivity between the DMN and SMN. The DMN and SMN negatively interact such that the activation of one is mirrored by the inactivation of the other (20).

Motor impairment is one of the most common complications reported in stroke survivors (26, 27). However, the underlying mechanisms of recovery remain not well understood. Various fMRI studies have shown the complexity of the process involved in motor function recovery (28–30). Several cross-sectional studies reported altered connectivity in brain networks after stroke, but only a handful of serial studies reported long term temporal changes (28, 31–34) and few have compared the temporal changes between ischemic and hemorrhagic stroke. In this longitudinal study, we compared the impact of IS and ICH on brain connectivity and their temporal changes over time using rsfMRI.

Methods And Procedures

Patient Enrollment & Human Protection

A total of 20 patients with intracerebral hemorrhage (ICH) and ischemic stroke (IS), 10 each, were admitted between 2012–2020 to Memorial Hermann Hospital and participated in a longitudinal imaging study. The images from 10 healthy volunteers images were downloaded from a public domain imaging database (<https://www.kennedykrieger.org/kirby-research-center/research/databases>). The study was approved by the institutional review board of the University of Texas Health Sciences Center at Houston and by the Memorial Hermann Hospital Office of Research. Written informed consent was obtained after a thorough discussion with patients and family members and all methods were performed in compliance to the approved study protocol. The inclusion-exclusion criteria included all patients diagnosed with IS or ICH age 18–80 years, hematoma volume or ischemic size < 100cc, NIHSS 0–20. Patients with a brain tumor, claustrophobia, or metal implantation were excluded.

Neurological and Radiological Assessments

All participants underwent baseline and serial assessment of neurological deficits using the National Institutes of Health Stroke Scale (NIHSS). The neurological assessments were correlated with the change

in neuronal connectivity between DMN and SMN. Baseline images (CT/MRI) were obtained within 6–24 hours of onset as part of the standard of care protocols. Follow-up imaging was obtained at 1, 3, and 12 months of ictus. The radiological assessments included lesion size, location, serial changes in hematoma, and edema volume.

Image Acquisition

Serial images were obtained on a full body 3.0 T Philips Inera later upgraded to Ingenia (Philips Medical Systems, Best, Netherland) system. Anatomical imaging included: 3D T1-weighted (TR/TE = 8.11/3.74 ms, imaging matrix = 256×256×180 mm³, slice thickness = 1 mm), and 3D fluid attenuated inversion recovery (FLAIR, TR/TE = 4800/129 ms, imaging matrix = 256×256×180 mm³, slice thickness = 1 mm). Resting-state blood oxygen level dependent (BOLD) functional MRIs (rsfMRI) (TR/TE = 2000/30 ms, FA = 8, dynamics = 120, voxel size = 2.75 x 2.75 x 3 mm) were obtained using echo planner imaging.

Lesion Volume Measurements

A semi-automated seed growing algorithm in Analyze 12.0 (Analyze Direct Inc., KS, USA) was used to measure hematoma and infarct volume on FLAIR images by a single rater. The rater selected a seed point within the infarct and a region-growing algorithm automatically expanded the seed points within the 3D space of the image. Manual editing was implemented when automated segmentation was not possible due to incongruent infarcts or if there were unclear lines of shape distinction with voxel intensities. For illustration purposes, all hematoma and infarct volumes were registered to the MNI brain template.

Resting-State fMRI

All patient lesions were aligned to the left hemisphere by flipping laterality. The connectivity analysis was performed using the CONN toolbox version 20.b (<https://web.conn-toolbox.org/>). All rsfMRI images were aligned and unwarped using SPM 12 (<https://www.fil.ion.ucl.ac.uk/spm/>). Subject motion was corrected after slice-time correction, wherein the data were time-shifted and resampled via sinc-interpolation to match the midpoint time of each acquisition. All scans were then co-registered to the first scan of each session using b-spline interpolation and centered to the (0,0,0) coordinates in all sessions. Potential outliers were identified as changes above five standard deviations or a frame-wise displacement above 0.9 mm (35–37). All functional and structural data files are normalized into standard MNI space and undergo grey matter, white matter, and CSF tissue segmentation. Brain volumes were extracted from the surrounding cranium as part of the segmentation and normalization process. Finally, the functional data undergoes data smoothing via spatial convolution with an 8 mm Gaussian kernel. Potential confounding effects to the BOLD signal in the white matter, CSF, realignment, scrubbing, and session effects were estimated and removed separately for each voxel in each functional data file using Ordinary Least Squares (OLS) regression. All BOLD signal time series were projected to the subspace orthogonal to all potential confounding effects.

Connectivity Analysis

Connectivity was evaluated using ROI-to-ROI group analysis by applying bivariate correlation and hemodynamic response function (hrf) weighting. The analysis utilizes ROIs constituting the Default Mode Network (DMN) and the Sensorimotor Network (SMN) as these two networks that previously has been reported in stroke patients (21, 23). The ROIs were taken from Harvard-Oxford and Automated Anatomical Labeling (AAL) atlases integrated within CONN functional connectivity toolbox. The connectivity analysis was performed in two separate groups. The first group compared IS patients and healthy control and the second group compared ICH patients to the healthy control. No direct comparison between IS and ICH was done due to lesion size and location variation. We also reported changes in individual patient's interconnectivity over time in each group. The average connectivity was analyzed to determine whether it differed from zero levels of the control group, with the p-values signify the false discovery rate (p-FDR).

Results

Demographics and Clinical Information

Imaging data from a total of 20 stroke patients and 10 healthy volunteers (70 scans) were used in this analysis. Each ischemic (4M/6F) and hemorrhagic (6M/4F) stroke group consisted of 10 participants with an average age of 55.9 ± 10.8 (range 35–75) and 55.3 ± 17.6 (range 29–78) years, respectively. Ten healthy volunteers (7M/3F) with an average age of 35.0 ± 12.1 (range 25–61) years were used as control at all three-time points. The median NIHSS of the ischemic group was significantly ($p < 0.05$) decreased from 5 (IQR = 3, 7) to 1 (IQR 0, 2) over one year. The median NIHSS of the ICH group was also significantly decreased ($p < 0.001$) from 4 (IQR 2, 11) to 1 (IQR 0, 2) over 12 months. Only one ICH patient underwent hemicraniectomy. Table 1 summarizes individual participant demographic data, overall lesion volume and hematoma volume at 1M, National Institute of Health Stroke Scale (NIHSS) at 1M, lesion/hemorrhage location, and lesion laterality.

Table 1
Demographics of sample groups.

	ID	Age	Gender	NIHSS	1M Lesion Volume (mm ³)	Lesion Location
Ischemic	1	35	F	7	43.60	Left Mesial Temporal, Occipital, Posterior Left Thalamus
	2	59	F	3	0.38	Pontine
	3	62	F	2	6.64	Right Occipital, Right PCA
	4	53	F	7	3.38	Left External Capsule
	5	46	M	3	6.93	Left Putamen
	6	59	F	11	80.20	Right Posterior Temporal Lobe
	7	57	M	5	0.55	Left Aspect of the Medulla
	8	61	M	6	3.95	Left, FL, PL, Pre Postcentral Gyri
	9	76	M	5	16.79	Left Occipital Lobe
	10	51	F	8	9.68	Right Caudate, External Capsule
	ID	Age	Gender	NIHSS	1M Lesion Volume (mm ³)	Lesion Location
Hemorrhagic	1	69	M	0	49.90	Left Parietal, Temporal Lobe
	2	64	M	4	7.85	Left Lentiform Nucleus, Ischemic insult Right Pontine
	3	67	F	13	7.42	Left Thalamus, PLIC, Centrum Semiovale
	4	54	M	3	13.98	Right Ventral Thalamus
	5	52	M	4	24.03	Left, FL, PL, Pre Postcentral Gyri
	6	33	M	14	68.24	Left Posterior Limb of Internal Capsule extending Superiorly and involving the Left Corona Radiata
	7	35	M	15	112.39	Left Posterior Temporal Lobe and Anterior Parietal Lobe
	8	29	F	2	99.38	Left Occipital Lobe

PCA = Posterior Cerebral Artery, FL = Frontal Lobe, PL = Parietal Lobe, PLIC = Posterior Limb of Internal Capsule.

ID	Age	Gender	NIHSS	1M Lesion Volume (mm ³)	Lesion Location
9	72	F	2	5.58	Right Basal Ganglia
10	78	F	6	10.50	Left Temporo-occipital Lobe

PCA = Posterior Cerebral Artery, FL = Frontal Lobe, PL = Parietal Lobe, PLIC = Posterior Limb of Internal Capsule.

Lesion Volume

There was no statistically significant difference between the hematoma and ischemic lesion volume ($p = 0.13$ at 1M) between the two groups at all three-time points. The average lesion volume of the ischemic group decreased from 17.2 ± 25.5 to 8.8 ± 11.2 mL ($p = 0.11$) over one year whereas in the ICH group the hematoma volume decreased from 39.9 ± 40.7 to 5.1 ± 7.9 mL ($p < 0.01$) over the same period. Figure 1 illustrates the average lesion size measured at 1 month of onset with all lesions flipped to the left hemisphere.

Connectivity

The changes in connectivity between the default mode and sensorimotor networks either within or between network ROIs are summarized in Fig. 2. The connectivity correlations are color-coded where warm colors represent positively correlated connections while cool colors represent negatively correlated connections. The healthy control group showed significant connectivity between the DMN and SMN (2A), whereas at 1M, both IS and ICH patients displayed no interaction between the two networks (2B, 2E). However, at 3M both IS and ICH patients exhibited a significant ($p\text{-FDR} > 0.01$) interaction whereby the IS group showed an increase among all three regions of the SMN to the left and right parietal regions of the DMN (2C) while ICH patients only displayed an increase in connectivity between the lateral right region of the SMN to the posterior cingulate cortex and left parietal regions of the DMN (2F). After one year, the IS group exhibited increased correlations in connectivity between the posterior cingulate cortex and left lateral motor cortex of the DMN, between the SMN's right cortex to the DMN's left and right parietal lobe, and between the SMN's superior motor cortex to the DMN's posterior cingulate cortex (2D). In comparison, the ICH patients at 12M exhibited increased interconnectivity between superior sensory-motor network to left and right lateral parietal regions of DMN, the medial prefrontal cortex of DMN to left and right lateral SMN, and lastly posterior cingulate cortex of DMN to lateral right of SMN (2G). The localized qualitative changes in the connectivity between DMN and SMN over time are displayed by brain surface mapping as shown in Fig. 3. As compared to 1M where each group exhibited no connectivity between DMN and SMN, at 12M, both IS and ICH patients showed an increase in a connectivity between DMN and SMN. The quantitative changes in connectivity between these two networks in each group are summarized in Table 2.

Table 2
Significant Connectivity Clusters amongst Ischemic and Hemorrhagic Stroke Patients (Computed at the zero level of a healthy control group).

	Ischemic Patients		Hemorrhagic Patients	
	F-Statistic	p-FDR	F-Statistic	p-FDR
01M				
SMN	29.79	0.000008	14.21	0.000354
DMN	25.95	0.000010	22.95	0.000044
03M				
SMN	103.08	0.000000	27.38	0.000011
DMN	22.05	0.000028	25.52	0.000011
Interconnectivity	5.06	0.018832	5.88	0.011429
12M				
SMN	129.62	0.000000	34.07	0.000003
DMN	27.88	0.000006	19.34	0.000063
interconnectivity	12.63	0.000435	6.50	0.008014

The average connectivity z-score change in individual ischemic and ICH patients over time is shown in Fig. 4 (A) and (B) respectively. Most of the patients in both IS and ICH exhibited a slight increase in z-scores between 1M and 3M, except for one IS and one ICH patient. However, the interconnectivity changes between 3M and 12M varied among individual participants. The overall average connectivity z-scores of three regions of the SMN in the IS group were higher than ICH patients at 1 month (red) which slightly decreased between 1 and 3 months then stabilized between 3 and 12 months as shown in Fig. 4 (C) and (D). Whereas ICH patients showed no change in average connectivity z-scores among the SMN regions. There was no significant temporal change exhibited by either IS or ICH patients in the average connectivity z-scores of the five DMN regions (blue). However, as compared to one month, both IS and ICH patients showed a significant increase in interconnectivity between the DMN and SMN at 3 and 12 months. There was no significant correlation between the change in interconnectivity and clinical outcome as measured on the NIHSS.

Discussion And Conclusions

In this longitudinal neuroimaging study, we compared post-stroke changes in neuronal connectivity in patients with ischemic versus hemorrhagic stroke. Several cross-sectional and serial connectivity imaging studies have been reported in patients with ischemic stroke (12, 18, 19, 22, 27). However, to the best of our knowledge, this is the first longitudinal imaging study that evaluated DMN and SMN connectivity in both hemorrhagic and ischemic stroke patients. Our results showed that regardless of stroke type, every

patient exhibited not only significant disruption in connectivity between the DMN and SMN, but also a global reduction among several brain networks. As compared to healthy controls, both ischemic and hemorrhagic stroke patients did not have expected negative correlations between the DMN and SMN at 1M. Furthermore, the decrease in connectivity in the positively correlated regions in the SMN and DMN were different between the two stroke types. For example, connectivity strength in the superior, left and right lateral SMN attenuated in the hemorrhagic patients, whereas it increased in ischemic stroke patients when compared to the healthy controls at 1M, as shown in Fig. 2. As compared to healthy controls, both IS and ICH patients exhibited a reduction in connectivity in most of the DMN regions at 1M. However, when comparing the two types of strokes, the ischemic patients had no connectivity between the medial prefrontal cortex and left lateral parietal regions of the DMN. The connectivity between the medial prefrontal cortex and posterior cingulate cortex was not affected in hemorrhage patients, but it decreased in ischemic patients. Connectivity between left and right parietal regions was unaffected in the ischemic stroke patients, but it decreased in hemorrhagic stroke. Our findings are in line with several post-stroke connectivity studies that reported acute decline or disruption in global connectivity regardless of ischemic or hemorrhagic stroke severity. However, Liu et al 2020 reported that this disruption in connectivity varies with ischemic lesion location. (22, 38–40)

The variance in interconnectivity change in individual participants substantiates the role of lesion size and location as shown in one of the IS patients (P06) with the biggest lesion volume who exhibited no improvement in interconnectivity over time. Another IS patient (P02) with the smallest pontine lesion showed a significant improvement in interconnectivity between 1M and 3M and then declined between 3M and 12M. Interestingly, one of the ICH patients (P2), who also developed an ischemic pontine lesion between 1M and 3M showed an opposite interconnectivity change as compared to the IS patient (P02). It is difficult to explain or speculate about the reasons for these changes due to pontine lesion. Temporally, both IS and ICH patients displayed an increase in negatively correlated connectivity between the DMN and SMN. However, this increase varied between the two types of stroke. The ischemic stroke patients displayed far more interconnectivity between the two networks as compare to hemorrhagic patients. The ischemic stroke patients exhibited strong connectivity between the left and right parietal region of the DMN to the left lateral sensory-motor, which was not observed in hemorrhagic stroke patients at 12 months. The hemorrhagic patents also lacked a connection between the right parietal and right sensory-motor cortex. Interestingly, as compared to IS patients, despite a significant reduction in hematoma volume, ICH patients exhibited a lesser magnitude of connectivity at 12M. However, our results are in contrast with a previous serial study that reported a significant increase in interhemispheric connectivity in hemorrhagic stroke as compared to ischemic stroke over 6 months (41). These differences could be due to lesion size, location, or different seed regions. This prior study investigated connectivity between the interior frontal cortex and motor-related regions whereas we investigated changes between the SMN and DMN. However, this variation in connectivity among studies could be due to several key factors such as age, gender, stroke severity, inclusion of both hemorrhagic and ischemic stroke, lesion size, and location, etc. Most of these studies including ours have small sample sizes.

In patients with ischemic stroke, our results are consistent with a previous longitudinal study that reported an increase in synchronization between the DMN and SMN after rehabilitation (21). Overall, the most consistent finding was the significant disruption in both local and global brain network connectivity in the acute phase, which strengthens during post-stroke recovery (19, 22, 23, 38); however, the role of interhemispheric connectivity remains controversial. Our data showed an increase in both inter and intrahemispheric connectivity whereas Park et al 2013 reported higher ipsilesional connectivity in the frontal and parietal cortices while Jungsoo Lee et al 2018 reported no change in intrahemispheric connectivity after stroke (33, 41, 42).

In conclusion, both IS and ICH stroke patients exhibited interconnectivity disruption between the DMN and SMN despite differences in pathology and location between the types of injuries. The restoration of the connectivity between these two networks was more prominent in ischemic stroke patients. Despite a significant decrease in hematoma volume as compared to the infarct lesion volume, ICH patients showed a weaker interaction between the DMN and SMN after one year. More detailed clinical assessments will be necessary in future studies to assess the clinical impact of disruption and restoration on interconnectivity between the DMN and SMN.

Declarations

Acknowledgement

The authors thank Mr. Vipulkumar Patel for imaging protocol setup and help with MRI experiments and Ms. Dorothea Parker for helping patient's recruitment and consent.

Author Contributions

Seth Boren: Data analysis, created Figures, plots, and drafted manuscript.

Muhammad E. Haque: Concept and design, data analysis and interpretation, writing manuscript.

Sean I. Savitz: Financial support, concept and design, data interpretation, writing manuscript.

Timothy Elimore: Reviewed data analysis, results interpretation, and edited manuscript.

Sarah George: Provision of study and patients recruitment

Octavio D. Arevalo: Radiological assessment, data analysis

Christin Silos: Statistical analysis

Maria Parekh: patients recruitment, reviewed and edit manuscript

Conflict of Interest

All the authors declared no conflict of interest directly related to this work.

Data Availability:

The datasets generated in this study are available from the corresponding author on reasonable request

References

1. Benjamin, E. J. *et al.* Heart Disease and Stroke Statistics-2019 Update: A Report From the American Heart Association., **139** (10), e56–e528 (2019).
2. Virani, S. S. *et al.* Heart Disease and Stroke Statistics-2020 Update: A Report From the American Heart Association., **141** (9), e139–e596 (2020).
3. Pinho, J., Costa, A. S., Araújo, J. M., Amorim, J. M. & Ferreira, C. Intracerebral hemorrhage outcome: A comprehensive update. *Journal of the neurological sciences*, **398**, 54–66 (2019).
4. Chae, J., Zorowitz, R. D. & Johnston, M. V. Functional outcome of hemorrhagic and nonhemorrhagic stroke patients after in-patient rehabilitation. *American journal of physical medicine & rehabilitation*, **75** (3), 177–182 (1996).
5. Paolucci, S. *et al.* Functional outcome of ischemic and hemorrhagic stroke patients after inpatient rehabilitation: a matched comparison., **34** (12), 2861–2865 (2003).
6. Perna, R. & Temple, J. Rehabilitation Outcomes: Ischemic versus Hemorrhagic Strokes. *Behavioural neurology*, **2015**, 891651 (2015).
7. Alawieh, A., Zhao, J. & Feng, W. Factors affecting post-stroke motor recovery: Implications on neurotherapy after brain injury. *Behavioural brain research*, **340**, 94–101 (2018).
8. Arya, K. N., Pandian, S., Kumar, D. & Puri, V. Task-Based Mirror Therapy Augmenting Motor Recovery in Poststroke Hemiparesis: A Randomized Controlled Trial. *Journal of stroke and cerebrovascular diseases: the official journal of National Stroke Association*, **24** (8), 1738–1748 (2015).
9. Hallam, G. P. *et al.* Task-based and resting-state fMRI reveal compensatory network changes following damage to left inferior frontal gyrus. *Cortex; a journal devoted to the study of the nervous system and behavior*, **99**, 150–165 (2018).
10. Jing, Y. H. *et al.* Comparison of Activation Patterns in Mirror Neurons and the Swallowing Network During Action Observation and Execution: A Task-Based fMRI Study. *Frontiers in neuroscience*, **14**, 867 (2020).
11. Rehme, A. K., Eickhoff, S. B., Wang, L. E., Fink, G. R. & Grefkes, C. Dynamic causal modeling of cortical activity from the acute to the chronic stage after stroke. *NeuroImage*, **55** (3), 1147–1158 (2011).
12. Rehme, A. K., Fink, G. R., von Cramon, D. Y. & Grefkes, C. The role of the contralesional motor cortex for motor recovery in the early days after stroke assessed with longitudinal FMRI. *Cerebral cortex* (New York, NY: 1991) **2011**;21(4):756–768.
13. Ogawa, S., Lee, T. M., Kay, A. R. & Tank, D. W. Brain magnetic resonance imaging with contrast dependent on blood oxygenation. *Proceedings of the National Academy of Sciences of the United*

States of America, **87** (24), 9868–9872 (1990).

14. Dennis, E. L. & Thompson, P. M. Functional brain connectivity using fMRI in aging and Alzheimer's disease. *Neuropsychology review*, **24** (1), 49–62 (2014).
15. Guerra-Carrillo, B., Mackey, A. P. & Bunge, S. A. Resting-state fMRI: a window into human brain plasticity. *The Neuroscientist: a review journal bringing neurobiology, neurology and psychiatry*, **20** (5), 522–533 (2014).
16. Polosecki, P. *et al.* Resting-state connectivity stratifies premanifest Huntington's disease by longitudinal cognitive decline rate. *Scientific reports*, **10** (1), 1252 (2020).
17. Sidhu, M. K., Duncan, J. S. & Sander, J. W. Neuroimaging in epilepsy. *Current opinion in neurology*, **31** (4), 371–378 (2018).
18. Grefkes, C. & Fink, G. R. Reorganization of cerebral networks after stroke: new insights from neuroimaging with connectivity approaches. *Brain: a journal of neurology*, **134** (Pt 5), 1264–1276 (2011).
19. Grefkes, C. & Ward, N. S. Cortical reorganization after stroke: how much and how functional? *The Neuroscientist: a review journal bringing neurobiology, neurology and psychiatry*, **20** (1), 56–70 (2014).
20. Huang, S. *et al.* Multisensory Competition Is Modulated by Sensory Pathway Interactions with Fronto-Sensorimotor and Default-Mode Network Regions. *The Journal of neuroscience: the official journal of the Society for Neuroscience*, **35** (24), 9064–9077 (2015).
21. Wu, C. W. *et al.* Synchrony Between Default-Mode and Sensorimotor Networks Facilitates Motor Function in Stroke Rehabilitation: A Pilot fMRI Study. *Frontiers in neuroscience*, **14**, 548 (2020).
22. Tuladhar, A. M. *et al.* Default Mode Network Connectivity in Stroke Patients. *PloS one*, **8** (6), e66556 (2013).
23. Chen, H. *et al.* Different Patterns of Functional Connectivity Alterations Within the Default-Mode Network and Sensorimotor Network in Basal Ganglia and Pontine Stroke. *Medical science monitor: international medical journal of experimental and clinical research*, **25**, 9585–9593 (2019).
24. Mak, L. E. *et al.* The Default Mode Network in Healthy Individuals: A Systematic Review and Meta-Analysis. *Brain connectivity*, **7** (1), 25–33 (2017).
25. Otti, A. *et al.* [Default mode network of the brain. Neurobiology and clinical significance], **83** (1), 1618–1624 (2012).
26. Carey, L. M. *et al.* Relationship between touch impairment and brain activation after lesions of subcortical and cortical somatosensory regions. *Neurorehabilitation and neural repair*, **25** (5), 443–457 (2011).
27. Dhand, A. *et al.* Social Network Mapping and Functional Recovery Within 6 Months of Ischemic Stroke. *Neurorehabilitation and neural repair*, **33** (11), 922–932 (2019).
28. Golestani, A. M., Tymchuk, S., Demchuk, A. & Goodyear, B. G. Longitudinal evaluation of resting-state FMRI after acute stroke with hemiparesis. *Neurorehabilitation and neural repair*, **27** (2), 153–163

- (2013).
29. Wang, L. *et al.* Dynamic functional reorganization of the motor execution network after stroke. *Brain: a journal of neurology*, **133** (Pt 4), 1224–1238 (2010).
 30. Xu, H. *et al.* Contribution of the resting-state functional connectivity of the contralesional primary sensorimotor cortex to motor recovery after subcortical stroke. *PloS one*, **9** (1), e84729 (2014).
 31. Hu, J. *et al.* Dynamic Network Analysis Reveals Altered Temporal Variability in Brain Regions after Stroke: A Longitudinal Resting-State fMRI Study. *Neural plasticity* 2018;2018:9394156.
 32. Ovadia-Caro, S. *et al.* Longitudinal effects of lesions on functional networks after stroke. *Journal of cerebral blood flow and metabolism: official journal of the International Society of Cerebral Blood Flow and Metabolism*, **33** (8), 1279–1285 (2013).
 33. Park, C. H. *et al.* Longitudinal changes of resting-state functional connectivity during motor recovery after stroke., **42** (5), 1357–1362 (2011).
 34. Tombari, D. *et al.* A longitudinal fMRI study: in recovering and then in clinically stable sub-cortical stroke patients. *NeuroImage*, **23** (3), 827–839 (2004).
 35. Esteban, O. *et al.* fMRIPrep: a robust preprocessing pipeline for functional MRI. *Nature methods*, **16** (1), 111–116 (2019).
 36. Parker, D. B. & Razlighi, Q. R. The Benefit of Slice Timing Correction in Common fMRI Preprocessing Pipelines. *Frontiers in neuroscience*, **13**, 821 (2019).
 37. Power, J. D. *et al.* Methods to detect, characterize, and remove motion artifact in resting state fMRI. *NeuroImage*, **84**, 320–341 (2014).
 38. Bonkhoff, A. K. *et al.* Acute ischaemic stroke alters the brain's preference for distinct dynamic connectivity states. *Brain: a journal of neurology*, **143** (5), 1525–1540 (2020).
 39. Lipson, D. M. *et al.* Recovery from stroke: differences between subtypes. *International journal of rehabilitation research Internationale Zeitschrift fur Rehabilitationsforschung Revue internationale de recherches de readaptation*, **28** (4), 303–308 (2005).
 40. Liu, H. *et al.* Patterns of motor recovery and structural neuroplasticity after basal ganglia infarcts. *Neurology*, **95** (9), e1174–e1187 (2020).
 41. Lee, J. *et al.* Alteration and Role of Interhemispheric and Intrahemispheric Connectivity in Motor Network After Stroke. *Brain topography*, **31** (4), 708–719 (2018).
 42. Buetefisch, C. M. Role of the Contralesional Hemisphere in Post-Stroke Recovery of Upper Extremity Motor Function. *Frontiers in neurology*, **6**, 214 (2015).

Figures

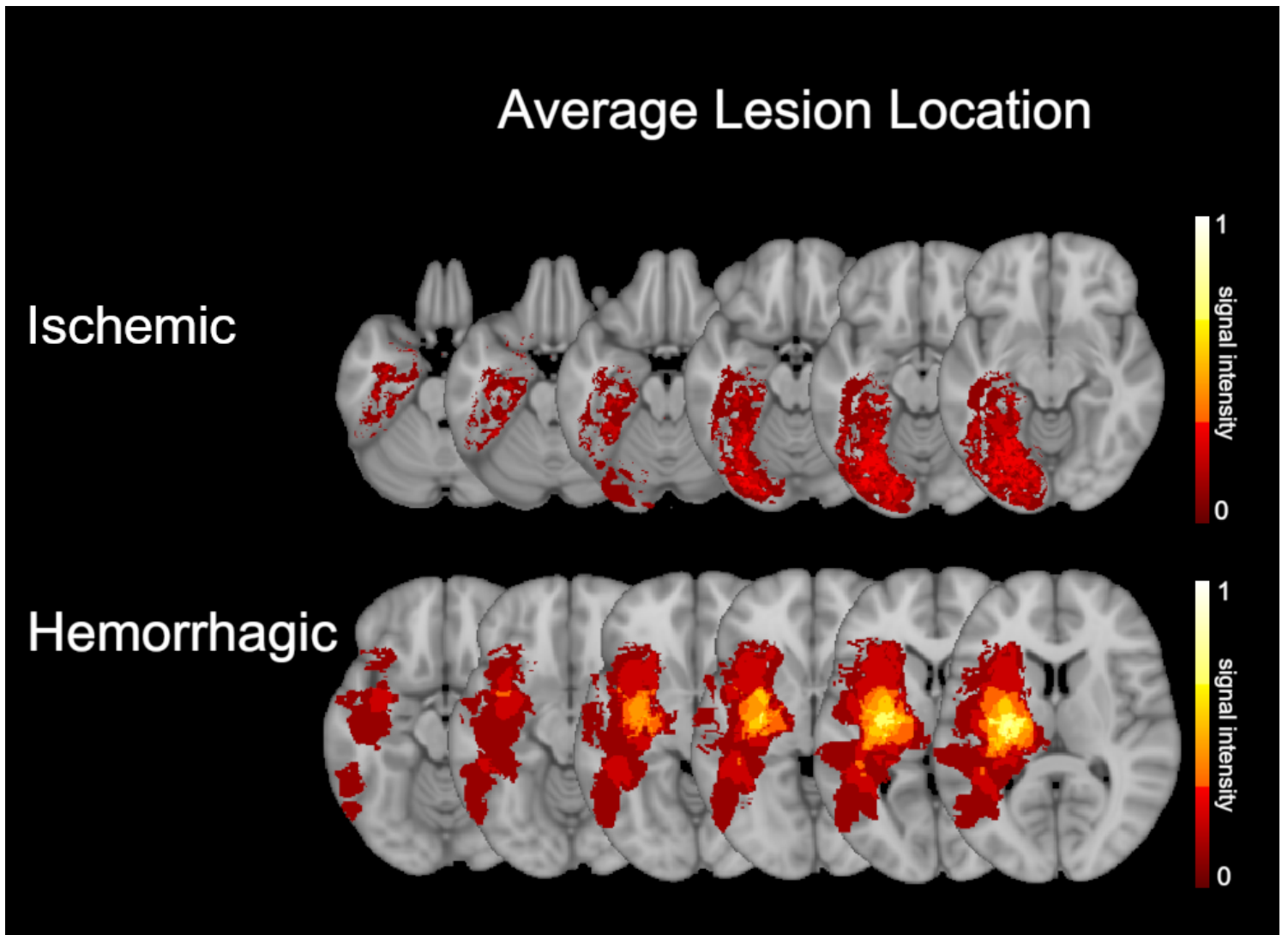


Figure 1

Average lesion volume mask in the ischemic and hemorrhagic stroke patients. The color bar represents variation in lesion signal intensities.

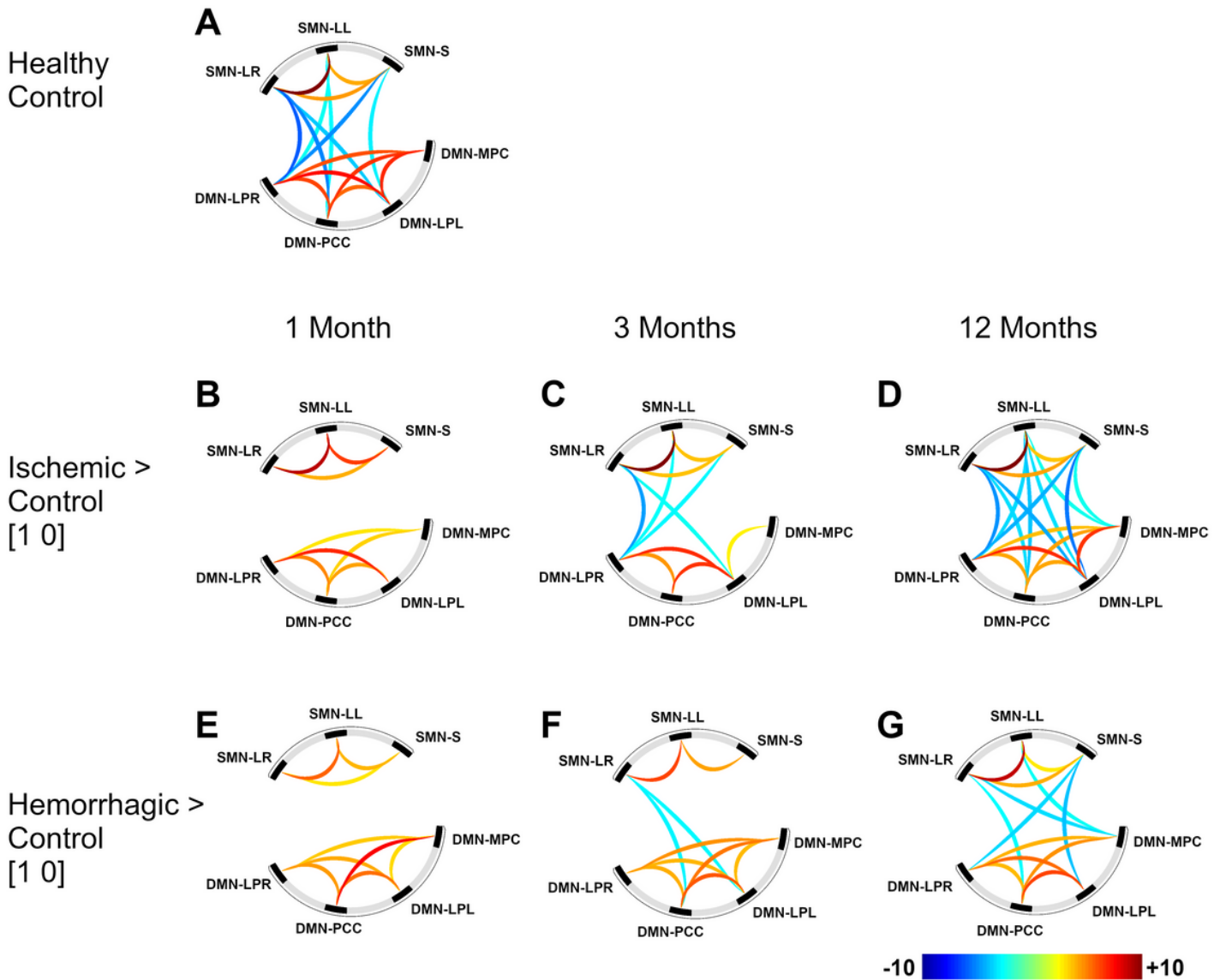


Figure 2

Summary of changes in the connectivity between default mode network (DMN) and sensorimotor network (SMN) at 1, 3, and 12 months in ischemic and hemorrhagic stroke patients. The color bar represents the magnitude of t-statistics between the seed and region of interest (ROI) illustrated by the range of positive (warm color) and negative (cool color) correlation change between the two networks over time. The first row illustrates the interconnectivity between DMN and SMN in healthy volunteers at one time point, whereas rows 2 and 3 are displaying temporal change in connectivity between the DMN and SMN network in the ischemic and hemorrhagic stroke patients respectively. Both ischemic and hemorrhagic stroke patients showed a significant ($p\text{-FDR} < 0.05$) increase in correlation between these two networks over one year.

Left Hemisphere Seeded from Default Mode Network Right Parietal

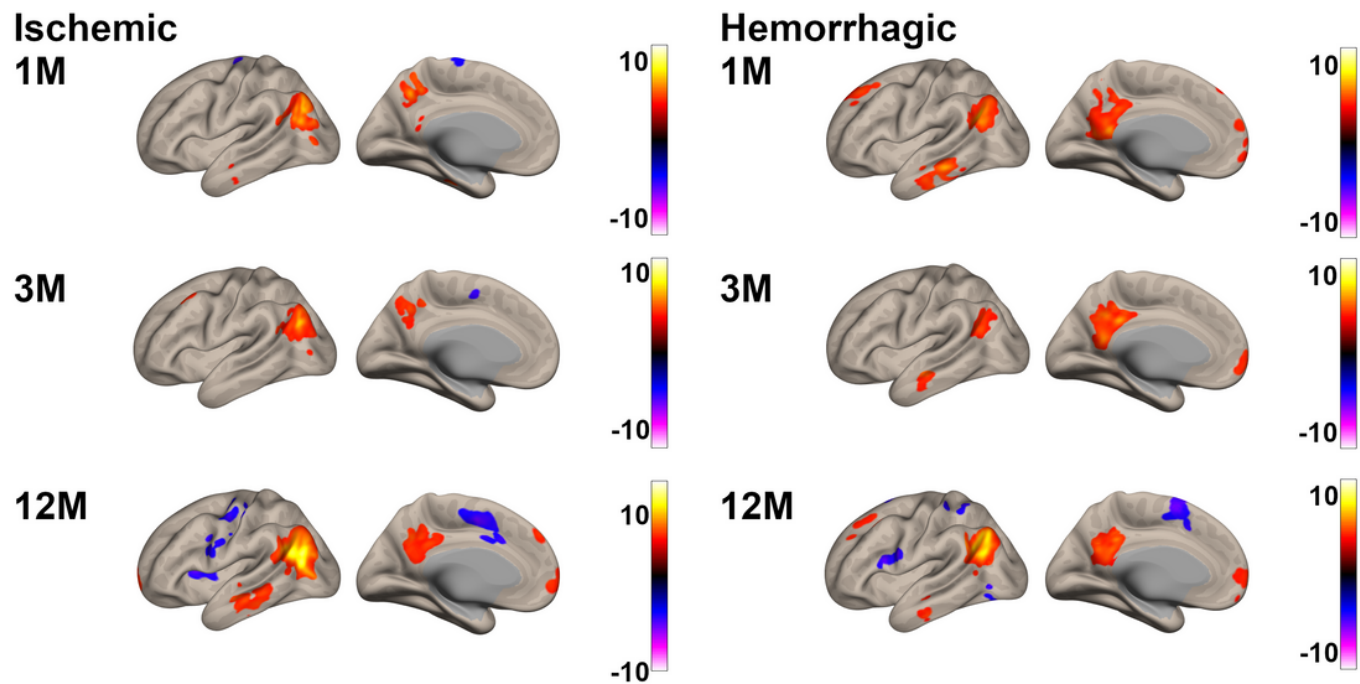


Figure 3

A surface plot of the lateral and medial view of the left (ipsilesional) hemisphere in ischemic and hemorrhagic stroke patients at 1, 3, and 12 months. Colored areas represent regions of significant connectivity seeded from the Default Mode Network Parietal Region of the right (contralesional) hemisphere. The color bar scale representing the positive and negative correlation z-scores. As compared to the one-month, the negative correlation between the DMN and SMN was significantly ($p\text{-FDR} < 0.05$) increased in both the ischemic and hemorrhagic stroke patients at 12 months.

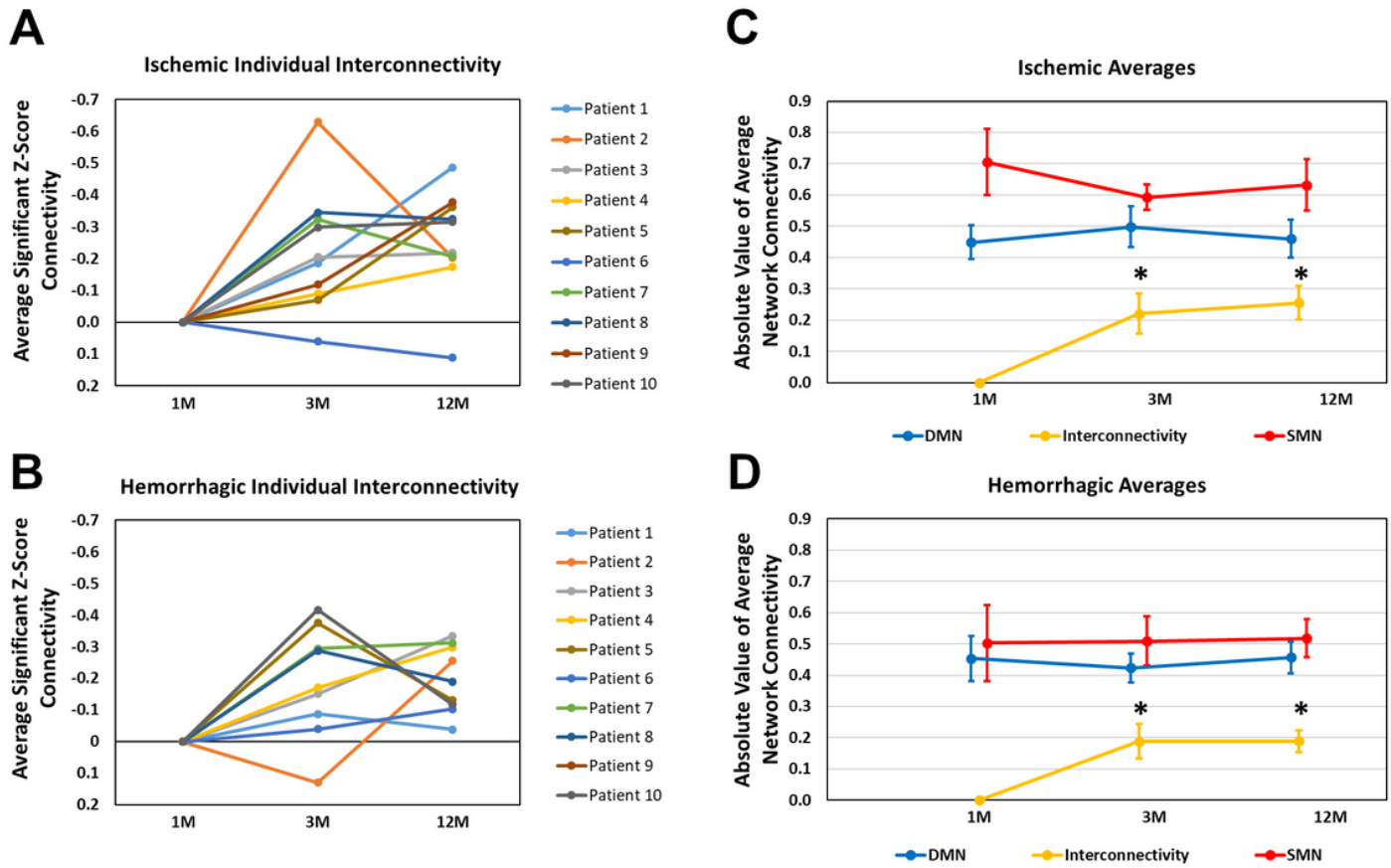


Figure 4

Changes in average connectivity z-scores in three regions of SMN, five regions of DMN, and interconnectivity in individual patients and overall at 1, 3, and 12 months of both ischemic and hemorrhagic stroke patients. The change in individual patients interconnectivity vary in both IS and ICH group as shown in A and B respectively. Overall, the IS patients (C) had a higher ($p < 0.05$) average connectivity z-score in the SMN as compared to the ICH (D) patients at one month, but decreased at 3 months and then stabilized. The changes in average connectivity z-scores in five regions of DMN remain unchanged in both the IS and ICH patients. The interconnectivity between SMN and DMN increase in both the IS and ICH patients.